The dynamic characteristics of a valve-less micropump*

Jiang Dan(蒋 丹)[a)†] and Li Song-Jing(李松晶)[b)]

[a)] School of Mechatronics Engineering, University of Electronic Science and Technology of China, Chengdu 611731, China

[b)] Department of Fluid Control and Automation, Harbin Institute of Technology, Harbin 150001, China

(Received 6 November 2011; revised manuscript received 3 January 2012)

The aim of this paper is to investigate the dynamic characteristics of a valve-less micropump. A dynamic mathematical model of the micropump based on a hydraulic analogue system and a simulation method using AMESim software are developed. By using the finite-element analysis method, the static analysis of the diaphragm is carried out to obtain the maximum deflection and volumetric displacement. Dynamic characteristics of the valve-less micropump under different excitation voltages and frequencies are simulated and tested. Because of the discrepancy between simulation results and experimental data at frequencies other than the natural frequency, the revised model for the diaphragm maximum volumetric displacement is presented. Comparison between the simulation results based on the revised model and experimental data shows that the dynamic mathematical model based on the hydraulic analogue system is capable of predicting dynamic characteristics of the valve-less micropump at any excitation voltage and frequency.

Keywords: valve-less micropump, dynamic characteristics, hydraulic analogue model, diffuser

PACS: 47.80.Fg, 47.85.Dh **DOI:** 10.1088/1674-1056/21/7/074701

1. Introduction

In the microfluid control system, a valve-less micropump is a necessary component. It has the ability to pump a wide variety of fluids automatically and accurately on a micro scale.[1−6] The dynamic characteristics of a valve-less micropump influence the performance of the microfluid control system. Consequently, it is of great importance to be able to accurately predict the dynamic characteristics of micropumps for appropriate design and usage of the microfluid control system.

The dynamic characteristic analysis of micropumps can be performed by using finite-element analysis (FEA) software, such as ANSYS[7] and FLUENT. However, increasing the complexity of the micropump structure or decreasing the size of the mesh elements makes the FEA methods time-consuming. Van der Pol *et al.*[8] used a bond-graphs method to model thermopneumatic micropumps. Olsson *et al.*[9,10] proposed a lumped-mass model to study the dynamic characteristics of valve-less diffuser micropumps.

The performance experiments for valve-less micropumps, including measurements of maximum pump pressure and capacity, have been performed by a number of authors.[11−15] However, investigations into the dynamic characteristics of valve-less micropumps have seldom been made. Zengerle and Richter[16,17] undertook transient pressure measurements of a pneumatically or electrostatically driven micropump with passive check valves. A 800-μm-wide and 0.4-μm-thick silicon carbide diaphragm was fitted on the pump chamber. The deflection of the silicon carbide diaphragm was detected by the pressure measurements with an optical test system.

In this paper, the dynamic characteristics of a piezoelectric valve-less micropump with nozzle/diffusers is studied theoretically and experimentally. On the basis of principle analogies between micropump elements and hydraulic components, the piezoelectric valve-less micropump is equivalent to a hydraulic model. By virtue of the AMESim software, a hydraulic analogue model is solved to predict the dynamic chamber pressure and the outlet flow rate of the micropump. The experimental data of the pressure pulsations in the valve-less micropump chamber

*Project supported by the Scientific Research Foundation for the Returned Overseas Chinese Scholars, Ministry of Education of China (Grant No. 24403604) and the Fundamental Research Funds for the Central Universities, China (Grant No. ZYGX2011J083).

†Corresponding author. E-mail: jdan2002@uestc.edu.cn

© 2012 Chinese Physical Society and IOP Publishing Ltd

under different excitation voltages and frequencies are compared with the corresponding simulation results.

2. Dynamic mathematical models

A typical schematic of a piezoelectric valve-less micropump is shown in Fig. 1. The micropump is composed of a pump chamber, nozzle/diffusers, a vibrated diaphragm, an inlet tube and an outlet tube.

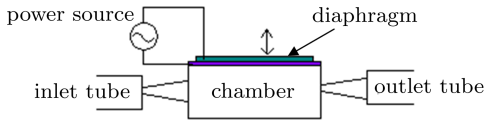
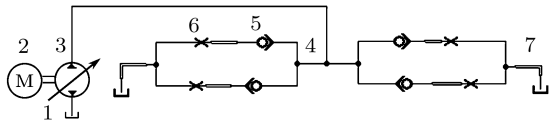


Fig. 1. (colour online) Schematic of the piezoelectric valve-less micropump with diffusers.

According to the principle analogies between micropump elements and hydraulic components, the whole hydraulic analogue model for the valve-less micropump is illustrated in Fig. 2. The external electric power source applied to the piezoelectric diaphragm can be equivalent to a hydraulic pump that pumps flow rate to a hydraulic system. It can be seen that the chamber can be replaced by a hydraulic junction with three ports. The nozzle and diffuser can be treated as elements having two different impedances in the forward and reverse directions. The inlet or outlet tube of the micropump can be equivalent to the pipeline in a hydraulic system.



1 reservoir, 2 electric motor, 3 pump,
4 hydraulic junction, 5 check valve,
6 hydraulic throttle valve, 7 pipe.

Fig. 2. Hydraulic analogue model for the micropump.

When constructing the hydraulic analogue model, it is assumed that:

1) the flow inside the system is unsteady and incompressible;

2) the external force and heat transfer are ignored.

The volumetric amplitude V of the vibrated diaphragm has a cosine character as

$$V = V_0[1 - \cos(\omega t)], \tag{1}$$

where V_0 is the maximum volumetric displacement of the diaphragm, and ω is the vibrated angular frequency. The time differential equation can be written as:

$$\frac{\mathrm{d}V}{\mathrm{d}t} = V_0\omega \sin(\omega t). \tag{2}$$

According to the mass conservation law, the flow-rate continuity equation for the micropump can be expressed as

$$\frac{\mathrm{d}V}{\mathrm{d}t} = q_\mathrm{i} - q_\mathrm{o}, \tag{3}$$

where q_i and qq_o are the inlet and outlet flow rate of the micropump, respectively. Thus,

$$q_\mathrm{i} - q_\mathrm{o} = V_0\omega \sin(\omega t). \tag{4}$$

The term $V_0\omega\mathrm{sin}(\omega\mathrm{t})$ in Eq. (4) can be replaced by the flow rate delivered by the hydraulic pump as shown in Fig. 2.

2.1. Model for the analogue throttle valve

As indicated in Fig. 2, the nozzle or diffuser is simply equivalent to sub-circuits made of a hydraulic throttle valve and a check valve linked in parallel. A hydraulic throttle valve represents the pressure loss through the nozzle or diffuser and a check valve represents the fluid flow direction in the nozzle or diffuser. The pressure loss Δp of the nozzle or diffuser can be expressed by the pressure loss over the hydraulic throttle valve as[14]

$$\Delta p = \frac{1}{2}\rho\xi\left(\frac{q}{A_\mathrm{n}}\right)^2, \tag{5}$$

where A_n is the cross section area of the hydraulic throttle valve, ρ is the fluid density, and ξ is the pressure loss coefficient of the valve. It shows the nonlinear flow-pressure characteristics of the throttle valve. q is the flow rate through the valve, which can then be written according to Eq. (5) as

$$q = A_\mathrm{n}\sqrt{\frac{2\Delta p}{\rho\xi}}. \tag{6}$$

2.2. Model for the analogue pipe

The Hagen–Poiseuille equation is used to describe the flow behavior in the inlet and outlet pipes. As the flow type in a pipe with a small cross-section area is

assumed to be a laminar flow, the fluid resistance $R_{\rm p}$ in the pipe can be described as[18]

$$R_{\rm p} = \frac{8\mu l}{\pi r^4}, \tag{7}$$

where μ is the dynamic viscosity of fluid, and l and r are the length and radius of the inlet or outlet pipe, respectively.

3. Static analysis of diaphragm

The vibrated diaphragm includes a piezoelectric membrane and a brass film. The piezoelectric membrane, made of PZT-5H, is glued on the brass film by epoxy. The radius and thickness of the piezoelectric membrane is 3.5 and 0.17 mm, respectively. The radius and thickness of the brass film is 6 and 0.17 mm, respectively. Here, the dimension of the epoxy can be ignored.

A static analysis of the vibrated diaphragm is performed using the FEA software ANSYS to obtain the maximum deflection and volumetric displacement. The vibrated diaphragm deflection influences the dynamic characteristics of the micropump. When a certain external voltage U is applied to the piezoelectric diaphragm, the structural displacement of the piezoelectric diaphragm along its polarization axis is the maximum deflection $x_{\rm max}$ in the middle of the vibrated diaphragm. According to the volume formula of a bell-shaped surface, the result of diaphragm volumetric displacement $V_{\rm sta}$ from the static analysis can be calculated. Table 1 provides the static-analysis results of the vibrated diaphragm under two different excitation voltages.

Table 1. Results from the static analysis.

	U/V$_{\rm p-p}$	$x_{\rm max}$/μm	$V_{\rm sta}$/ml
1st set	70	3.62	1.6×10^{-4}
2nd set	80	3.84	1.7×10^{-4}

4. Simulation results

The hydraulic analogue model is simulated by using the AMESim software under different driving voltages and frequencies. It is assumed that the flow rate of the pump in the hydraulic analogue model has a sine-type character. The maximum output flow rate of the hydraulic pump is $V_0\omega$. The maximum volumetric displacement of the vibrated diaphragm V_0 equals $V_{\rm sta}$. The value of $V_{\rm sta}$ can be obtained from the static-analysis results of the vibrated diaphragm. The pressures in the two reservoirs at the inlet and outlet keep constant ($p_{\rm in} = p_{\rm out} = 1 \times 10^5$ Pa). According to the construction parameters of the micropump listed in Table 2, the pressure loss coefficient of nozzle $\xi_{\rm n}$ and diffuser $\xi_{\rm d}$ are calculated to be 1 and 0.2.[19] The inlet or outlet pipe length l and radius r are 0.1 m and 1 mm, respectively.

Table 2. Construction parameters of the micropump.

Parameter	Value
Diffuser inlet width/μm	150
Diffuser outlet width/μm	570
Diffuser depth/μm	200
Diffuser length/mm	3
Chamber diameter/mm	10
Chamber depth/μm	500

In order to investigate the influences of excitation voltage and frequency, we conduct simulations for the excitation voltages of 70 V$_{\rm p-p}$ and 80 V$_{\rm p-p}$, and the frequencies of 200 and 300 Hz. The corresponding maximum volumetric displacement of the vibrated diaphragm V_0 is equal to 1.6×10^{-4} and 1.7×10^{-4} ml, respectively, which are obtained from the results listed in Table 1. The predicted results of the pressure in the pump chamber and the outlet flow rate obtained from the hydraulic analogue model are shown in Figs. 3(a) and 3(b), respectively.

At a frequency of 200 Hz, it can be seen from Fig. 3(a) that under the excitation of external voltage, the vibration of the diaphragm above the chamber results in pressure pulsations in the pump chamber. Under an excitation voltage of 70 V$_{\rm p-p}$, the calculated minimum chamber pressure is about 9.401×10^4 Pa during the 'supply' mode and the maximum is about 1.060×10^5 Pa during the 'pump' mode; under an excitation voltage of 80V$_{\rm p-p}$, the calculated minimum chamber pressure is about 9.323×10^4 Pa and the maximum is about 1.068×10^5 Pa. In particular, two turning points arise, where the chamber pressure $p_{\rm c}$ is equal to $p_{\rm out}$ and $p_{\rm in}$ between the 'supply' mode and the 'pump' mode.

As shown in Fig. 3(b), under an excitation voltage of 70 V$_{\rm p-p}$, the calculated maximum outlet flow rate is about -3.7×10^{-3} L/min during the 'supply' mode, and the maximum is about 8.3×10^{-3} L/min during the 'pump' mode; under an excitation voltage of 80 V$_{\rm p-p}$, the calculated maximum outlet flow rate is about -4.0×10^{-3} L/min during the 'supply' mode and the maximum is about 8.8×10^{-3} L/min during

the 'pump' mode. Because the outlet flow rate during the 'pump' mode is higher than that during the 'supply' mode, the fluid is transported out of the micropump.

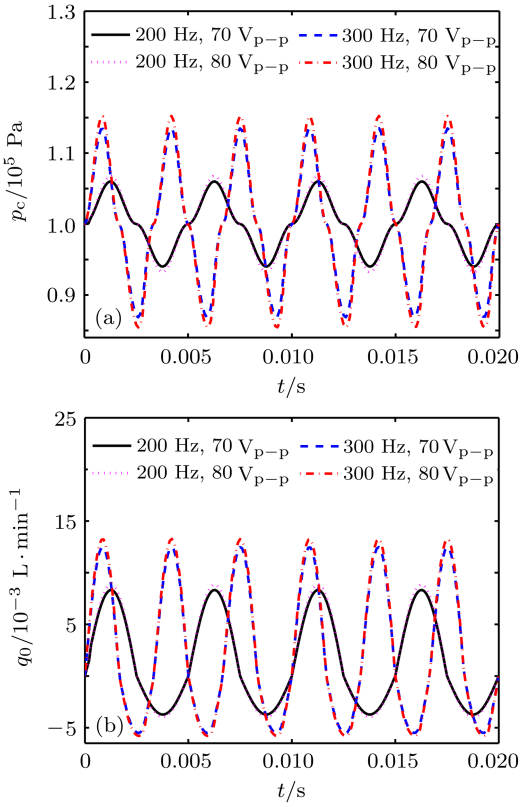


Fig. 3. (colour online) Simulation results of (a) pressure in the pump chamber and (b) outlet flow rate under different driving voltages and frequencies.

In Fig. 3(a), at a frequency of 300 Hz, the calculated amplitude of the chamber pressure is about 2.663×10^4 Pa under an excitation voltage of 70 V_{p-p}; the calculated amplitude of the chamber pressure is about 2.980×10^4 Pa under an excitation voltage of 80 V_{p-p}. In Fig. 3(b), under an excitation voltage of 70 V_{p-p}, the calculated amplitude of the outlet flow rate is about 1.80×10^{-2} L/min; under an excitation voltage of 80 V_{p-p}, the calculated amplitude of the outlet flow rate is about 1.91×10^{-2} L/min. Comparison of the simulation results between the excitation voltages of 70 V_{p-p} and 80 V_{p-p}, as well as that between the frequencies of 200 and 300 Hz show that the chamber pressure pulsations and outlet flow rate amplitudes decrease with decreasing excitation voltage and frequency.

5. Experimental investigation

Dynamic characteristics of the micropump have been tested in order to study the characteristics of the micropump and to verify the validity of the valve-less micropump mathematical model based on the hydraulic analogue system. Deionized water was used as the working fluid in the experiments. Figure 4 shows the actual dynamic experimental setup for the micropump. It mainly consists of a signal generator, a micropump, and a pressure sensor.

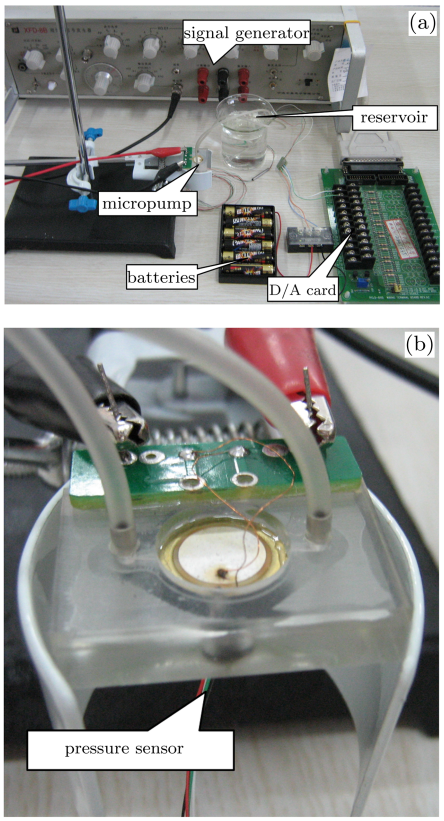


Fig. 4. (colour online) Photograph of the experimental setup. (a) The integrated graph. (b) Local figure.

The valve-less micropump was driven by a square wave from an XFD-8B signal generator. The amplitude and frequency of the square wave can be regulated. The signal generator provides an output voltage range from 0 to 250 V_{p-p} and a frequency range from 0.0005 to 10 kHz.

Figures 5(a) and 5(b) are the photographs of valve-less micropumps with and without the pressure sensor, respectively. The base material of the micropump is transparent polymethyl methacrylate (PMMA). Ultra-precision machining was used to fabricate the diffuser and chamber of the valve-less micropump. On the top of the pump chamber, the vibrated piezoelectric diaphragm was glued by epoxy.

The construction parameters of the micropump are listed in Table 2. During the experiments, the inlet and outlet of the micropump were all linked to the reservoir.

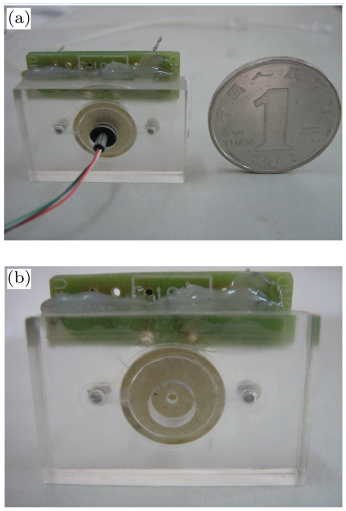


Fig. 5. (colour online) Photograph of the piezoelectric valve-less micropumps (a) with and (b) without a miniaturized pressure sensor.

As illustrated in Fig. 5(a), a miniaturized pressure sensor (XCL-080 by Kulite), fitted on the top of the pump chamber, was used to record the dynamic characteristics of the micropump chamber pressure. Here a black rubber O-ring acted as the sealing component. The pressure probe of the miniaturized pressure sensor has a diameter of 2 mm and a length of 6.4 mm. Its pressure range is from 0 to 1.7×10^5 Pa and its response frequency is 240 kHz. The electrical excitation to the pressure sensor was supplied by batteries with a DC voltage of 10 V. The computer with a D/A card (PCL-818HG by Advantech) acquires the output signal from the pressure sensor to achieve the dynamic pressure data acquisition.

The performance experiments of the valve-less micropump, including measurements of maximum pump pressure and capacity, have been conducted. The experimental results indicate that the micropump has a pump capacity of about 1400 μL/min and a maximum pump pressure of 1150 Pa when the diaphragm vibrates at the natural frequency f_0 of 250 Hz.

6. Comparison between simulation and experimental results

Table 3 lists six sets of parameters, including the excitation voltage U, the frequency f, and the diaphragm maximum volumetric displacement V_0. The V_0 is equal to $V_{\rm sta}$ obtained from the static-analysis results (Table 1). In Figs. 6–8, the simulation results of the pressure in the pump chamber obtained from the hydraulic analogue model using AMESim software are shown by dashed lines. The accuracy of the hydraulic analogue model is demonstrated by comparing the simulation results with the experimental results (solid line) under the same conditions.

Table 3. Static-analysis results of the excitation voltage, the frequency, and the diaphragm maximum volumetric displacement.

Set	$U/\mathrm{V_{p-p}}$	f/Hz	V_0/ml
1st	70	250	1.6×10^{-4}
2nd	80	250	1.7×10^{-4}
3rd	70	294	1.6×10^{-4}
4th	80	294	1.7×10^{-4}
5th	70	125	1.6×10^{-4}
6th	80	125	1.7×10^{-4}

In Figs. 6(a) and 6(b), the first and second sets of parameter values are used, respectively. The frequency is 250 Hz, which is the natural frequency (f_0) of the micropump. In Fig. 6(a), the experimental minimum chamber pressure is about 9.025×10^4 Pa and the maximum is about 1.097×10^5 Pa. It can be seen

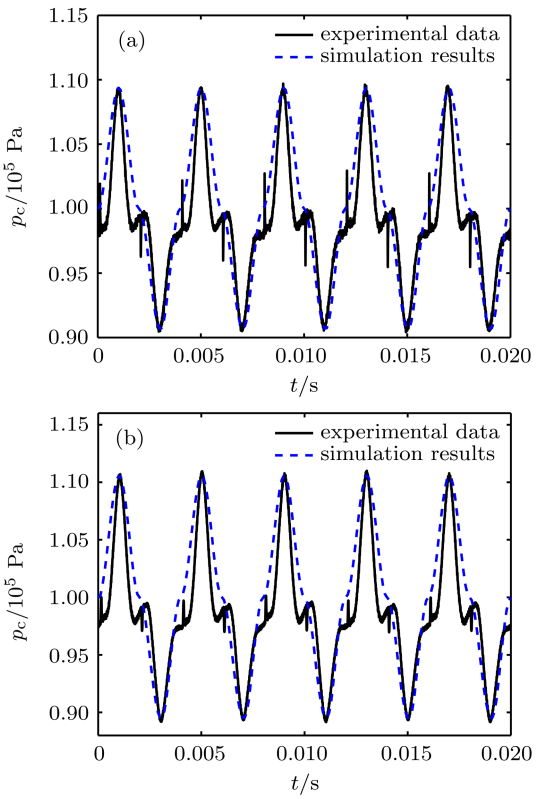


Fig. 6. (colour online) Comparison between simulation and experimental data under voltages of (a) 70 $\mathrm{V_{p-p}}$ and (b) 80 $\mathrm{V_{p-p}}$ at frequency of 250 Hz.

that the pump chamber pressure obtained from the hydraulic analogue model agrees well with the experimental results tested with the miniaturized pressure sensor. In particular, there are pressure shocks at the inversion point between the 'supply' mode and the 'pump' mode, which is similar to the piston pump instantaneous back-flow phenomenon because of the compressibility of fluid.[20] However, these effects are ignored in the analogue model of the valve-less micropump.

In Fig. 6(b), the experimental minimum chamber pressure is about 8.912×10^4 Pa and the maximum is about 1.110×10^5 Pa. As can be seen, there is a good agreement between the experimental pressure data and the simulation results.

In order to further verify the efficiency and practice of the hydraulic analogue model, the experiments for different driving frequencies have been carried out. In Fig. 7(a), the third set of parameter values in Table 3 is applied. Here the frequency is 294 Hz, which is different from the natural frequency of the micropump. The calculated minimum chamber pressure is about 8.736×10^4 Pa and the maximum is about 1.129×10^5 Pa. However, the experimental minimum chamber pressure is about 9.067×10^4 Pa and the maximum is about 1.092×10^5 Pa. Figure 7(a) shows that there is a difference between the values of pressure pulsation amplitude obtained from experiments and simulations.

In Fig. 7(b), the fourth set of parameter values is adopted. This figure suggests that the simulation results of pressure pulsation amplitude are larger than the experimental data. The calculated minimum chamber pressure is about 8.597×10^4 Pa and the maximum is about 1.146×10^5 Pa. However, the experimental minimum chamber pressure is about 9.036×10^4 Pa and the maximum is about 1.095×10^5 Pa. Comparison of the results demonstrates that when the driving frequency is higher than the natural frequency of micropump, the simulated maximum volumetric displacement of the vibrated diaphragm should be less than the analyzed volumetric displacement.

According to the fifth and sixth sets of parameter values in Table 3, when the diaphragm vibration frequency is 125 Hz, which is lower than the natural frequency, the comparisons between the simulation results and experimental data under the excitation voltages of 70 V_{p-p} and 80 V_{p-p} are illustrated in Figs. 8(a) and 8(b), respectively. It can be seen that

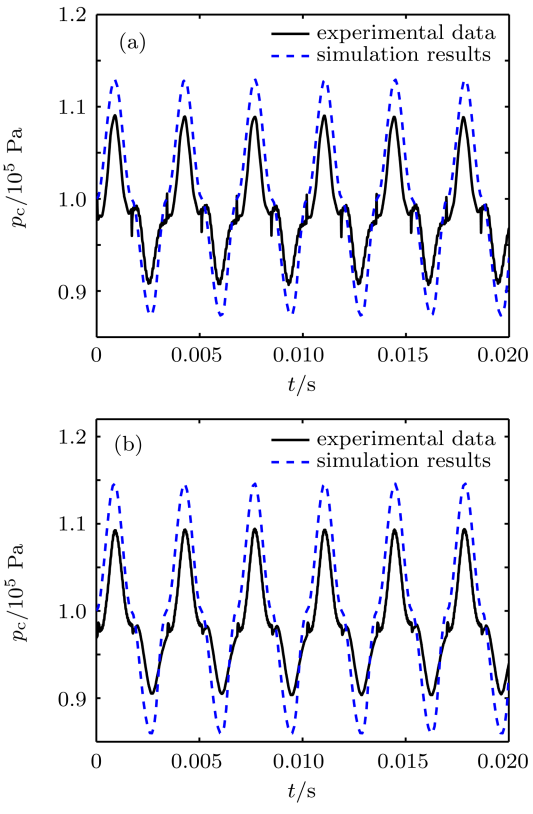


Fig. 7. (colour online) Comparison between simulation and experimental data under voltages of (a) 70 V_{p-p} and (b) 80 V_{p-p} at frequency of 294 Hz.

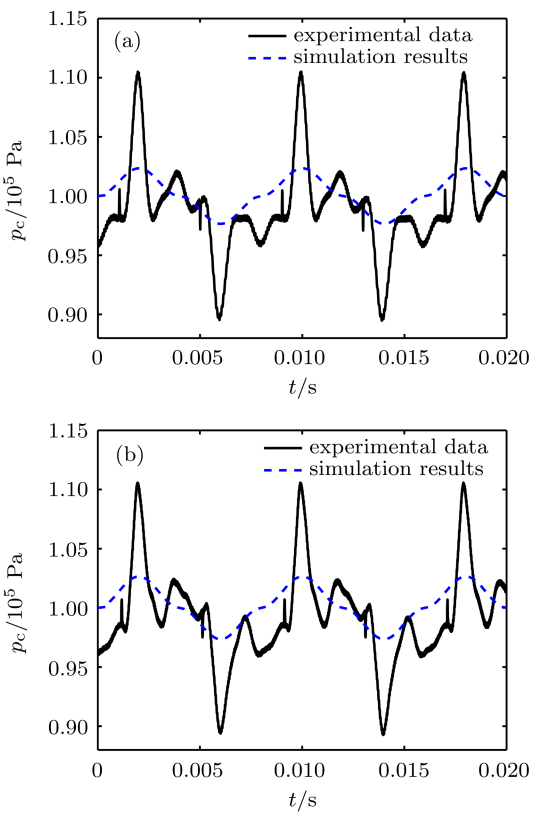


Fig. 8. (colour online) Comparison between simulation and experimental data under voltages of (a) 70 V_{p-p} and (b) 80 V_{p-p} at a frequency of 125 Hz.

the tested amplitudes of pressure pulsations are inconsistent with the simulation results. Comparison of the results demonstrates that when the driving frequency is lower than the natural frequency of the micropump, the simulated maximum volumetric displacement of the vibrated diaphragm should be larger than the analyzed volumetric displacement.

7. Revised model

From the above studies, it can be seen that the mathematical model of the vibrated diaphragm maximum volumetric displacement V_0 should be revised, especially at frequencies other than the natural frequency of the valve-less micropump.

Due to the influence of the diaphragm on the maximum deflection, the driving frequency should be taken into account in the calculation of the diaphragm maximum volumetric displacement. When the driving frequency is higher than the natural frequency, the vibrated diaphragm cannot reach the volumetric displacement obtained from the above static analysis. When the driving frequency is lower than the natural frequency, the vibrated diaphragm can exceed the volumetric displacement obtained from the static analysis. When the driving frequency is equal to the natural frequency, the tested displacement of the vibrated diaphragm can match the static-analysis results of the volumetric displacement. Therefore, the revised maximum volumetric displacement should be a function of the excitation frequency f. Thus, the value of V_0 becomes

$$V_0 = kV_{\rm sta}\frac{f_0}{f}, \tag{8}$$

where k is the revised coefficient, which is also a function of frequency.

As shown in Fig. 6, at the natural frequency f_0, the maximum volumetric displacement V_0 is equal to $V_{\rm sta}$, which has been proved by experiments. In Eq. (8), the value of the revised coefficient k should be chosen to be 1. Thus, $V_0 = V_{\rm sta}$ is a special case of Eq. (8).

At a frequency other than the natural frequency f_0, the values of the revised coefficient k can be calculated according to the pressure pulsation amplitudes under an excitation voltage of 80 V_{p-p}. The other tested pressure pulsations under an excitation voltage of 70 V_{p-p} are used to verify the validity of the revised model. The values of k are calculated to be 0.995, 1, and 0.951 for frequencies of 125, 250, and 294 Hz, respectively. It can be seen that the revised coefficient k has its maximum value at the natural frequency of the micropump. This means that at the natural frequency, the amplitude of the pressure pulsations is more than that at the other excitation frequencies. According to Eq. (6), the larger the pressure pulsation amplitude, the more the micropump outlet flow rate is. Thus, the micropump pressure and capacity have maximum values at the natural frequency.

Here, by taking three excitation frequencies as examples, the calculation method of the revised coefficient is presented. In regard to the value of the revised coefficient corresponding to another frequency, future work needs to be done.

As illustrated by Fig. 9(a), the excitation voltage is 80 V_{p-p} and the frequency is 125 Hz. The maximum volumetric displacement V_0 was changed from 1.7×10^{-4} to 3.383×10^{-4} ml. The tested chamber pressure pulsations (solid line) and the simulation results obtained from the revised model (dotted line) are shown in Fig. 9(a). It can be seen that the two curves agree well with each other.

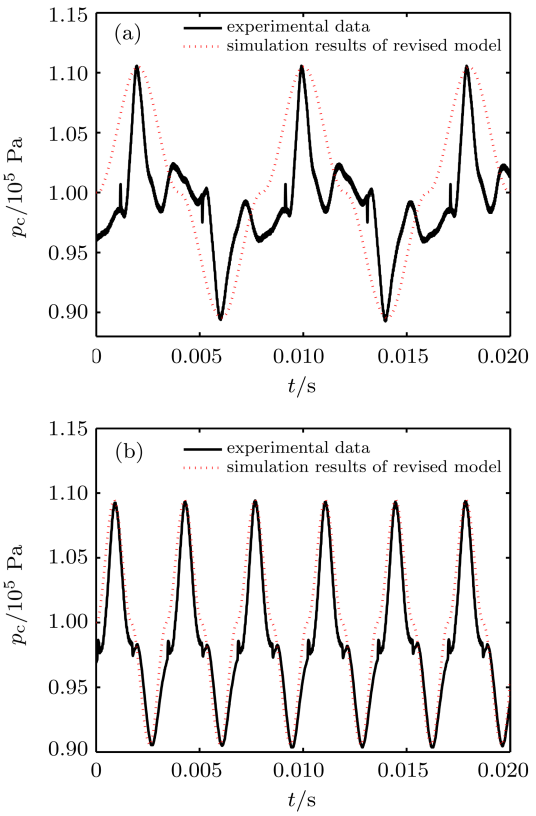


Fig. 9. (colour online) Comparison between the simulation results obtained from the revised model and the experimental data at frequencies of (a) 125 and (b) 294 Hz at an excitation voltage of 80 V_{p-p}.

At a frequency of 294 Hz, which is lower than the natural frequency, the comparison between the simulation results obtained from the revised model (dotted line) and the experimental data (solid line) under an excitation voltage of 80 V_{p-p} is illustrated in Fig. 9(b). According to Eq. (8), the revised maximum volumetric displacement is equal to 1.375×10^{-4} ml. After the revision, the simulation results of chamber pressure are in agreement with the experimental data.

In order to verify the accuracy of the revised coefficient, the simulation results obtained from the revised model using AMESim are compared with the corresponding experimental data at an excitation voltage of 70 V_{p-p}. As shown in Figs. 10(a) and 10(b), the driving frequencies are 125 and 294 Hz, respectively. According to Eq. (8) and the revised cofficient, at a frequency of 125 Hz, the maximum volumetric displacement V_0 increases from 1.6×10^{-4} to 3.184×10^{-4} ml; at a frequency of 294 Hz, the maximum volumetric displacement V_0 decreases from 1.6×10^{-4} to 1.294×10^{-4} ml. In Fig. 10, the tested chamber pressure pulsations are shown by a solid line and the simulation results obtained from the revised model are shown by a dotted line. It can be seen that the experimental data and the simulation results obtained from the revised model are in good agreement. In accordance with the comparison results, the feasibility of the micropump dynamic analysis with revised maximum volumetric displacement is verified.

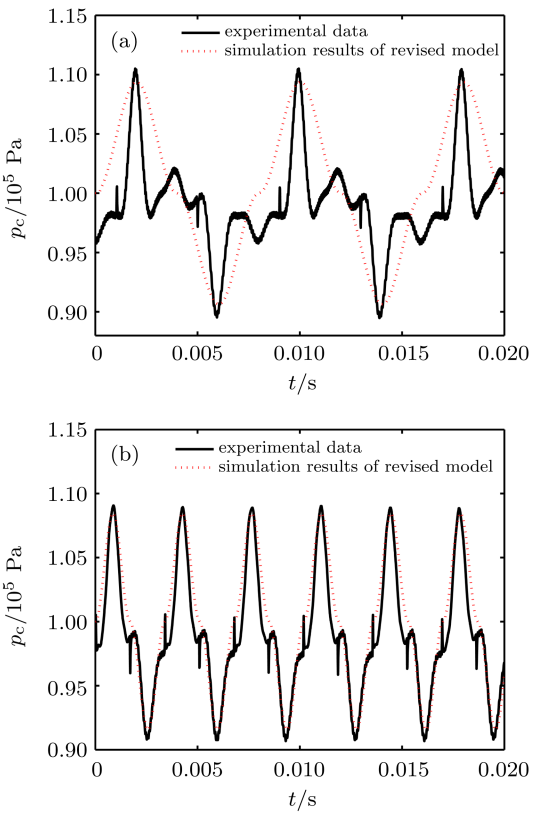


Fig. 10. (colour online) Comparison between the simulation results of the revised model and experimental data at frequencies of (a) 125 and (b) 294 Hz at an excitation voltage of 70 V_{p-p}.

8. Conclusions

In this paper, the dynamic characteristics of the piezoelectric valve-less diffuser micropump are investigated theoretically and experimentally. A dynamic mathematical model based on the hydraulic analogue system has been developed to predict the chamber pressure and the outlet flow rate of the valve-less micropump. The revised model for the diaphragm maximum volumetric displacement is given, which is a function of the excitation frequency. A comparison between the simulation results and the experimental data, obtained from the miniaturized pressure sensor fitted on the top of the chamber, shows that the usage of the revised maximum volumetric displacement results in a better prediction of chamber pressure pulsations at any excitation frequency.

Obviously, according to the comparison between the experimental data and the simulation results, there are discrepancies in the pressure pulsation amplitudes occurring at the inversion point between the 'supply' mode and the 'pump' mode due to instantaneous back-flow phenomenon in the micropump. Our next work is to further study the back-flow phenomenon and its influence on the dynamic characteristics of micropumps.

It should be noted that this study has examined only the pressure pulsations inside the valve-less micropump chamber. It is now necessary to conduct experiments to study the dynamic characteristics of the valve-less micropump outlet flow rate at different driving voltages and frequencies.

References

[1] Kan J W, Yang Z G, Peng T J, Cheng G M and Wu B D 2005 *Sens. Actuators* A **121** 156

[2] Andersson H, van der Wijngaart W, Nilsson P, Enoksson P and Stemme G 2005 *Sens. Actuators* A **122** 131

[3] Luo Z B and Xia Z X 2001 *Sens. Actuators* B **72** 259

[4] Gravesen P, Brandebjerg J and Jensen O S 1993 *J. Micromech. Microeng.* **3** 168

[5] Bourouina T, Bossebceuf A and Grandchamp J 1997 *J. Micromech. Microeng.* **7** 186

[6] Jiang D, Li S J and Bao G 2008 *Acta Phys. Sin.* **57** 5072 (in Chinese)

[7] Koch M, Evans A G R and Brunnschweiler A 1996 *Proc. Tech. Digest MME* September 3–5, 1995 Copenhagen, Denmark p. 160

[8] van de Pol F C M, Breedveld P C and Fuitman J H J 1990 *Proc. Tech. Digest MME* November 26–27, 1990 Berlin, Germany p. 19

[9] Olsson A, Stemme G and Stemme E 1999 *J. Micromech. Microeng.* **9** 34

[10] Olsson A, Stemme G and Stemme E 1995 *Sens. Actuators* A **46** 549

[11] Zhang H J and Qiu C J 2006 *Mater. Sci. Eng.* A **438** 1106

[12] Stemme E and Stemme G 1993 *Sens. Actuators* A **39** 159

[13] Schabmueller C G J, Koch M, Mokhtari M E, Evans A G R, Brunnschweiler A and Sehr H 2002 *J. Micromech. Microeng.* **12** 420

[14] Ullmann A 1998 *Sens. Actuators* A **69** 97

[15] Richter M, Linnemann R and Woias P 1998 *Sens. Actuators* A **68** 480

[16] Zengerle R, Geiger W, Richter M, Ulrich J, Kluge S and Richter A 1995 *Sens. Actuators* A **46** 557

[17] Zengerle R and Richter M 1994 *J. Micromech. Microeng.* **4** 192

[18] Bourouina T and Grandchamp J 1996 *J. Micromech. Microeng.* **6** 398

[19] Olsson A, Stemme G and Stemme E 2000 *Sens. Actuators* A **84** 165

[20] Furukawa A, Shigemitsu T and Watanabe S 2007 *J. Therm. Sci.* **16** 7